Available online at www.sciencedirect.com
ScienceDirect
Trans. Nonferrous Met. Soc. China 32(2022) 1548−1558
Transactions of Nonferrous Metals Society of China
www.tnmsc.cn

Microstructural evaluation of Hastelloy-X transient liquid phase bonded joints: Effects of filler metal thickness and holding time

A. MALEKAN[1], S. E. MIRSALEHI[2], M. FARVIZI[1], N. SAITO[3], K. NAKASHIMA[3]

1. Ceramic Division, Materials and Energy Research Center, P.O. Box 14155-4777, Tehran, Iran;
2. Department of Materials and Metallurgical Engineering,
Amirkabir University of Technology (Tehran Polytechnic), Tehran 15875-4413, Iran;
3. Department of Materials Science and Engineering, Kyushu University, 744, Motooka, Nishi-ku,
Fukuoka 819-0395, Japan

Received 9 May 2021; accepted 15 November 2021

Abstract: Transient liquid phase (TLP) bonding was investigated in Hastelloy-X samples with different filler metal thicknesses (20, 35, 50, 65, and 100 μm) and holding time (5, 20, 80, 320, and 640 min) to obtain optimum bonding parameters. Microstructural evaluations using electron probe microanalysis (EPMA) and electron backscattered diffraction (EBSD) show that the central eutectic phases present in the athermally solidified zone (ASZ) are Ni_3B, Ni_2Si, and CrB, and the precipitates formed in the diffusion-affected zone (DAZ) are MoB, CrB_2, and Mo_2B_5. According to the results, decreasing the filler thickness as well as increasing the holding time helps realize the completion of isothermal solidification and reduction in the density of precipitates in the DAZ, leading to a joint with more uniform properties. Diffusion of boron and silicon to longer distances with increasing holding time causes the removal of Cr-rich borides in the DAZ and the formation of Mo-rich silicide at the joint interface. Decrease in hardness of ASZ and DAZ due to the elimination of brittle phases in these zones during long holding time causes more uniform hardness distribution in the joint area. The best results are obtained for the sample joined with the 35 μm-thick filler metal for 640 min holding time.

Key words: Hastelloy-X; transient liquid phase (TLP) bonding; microstructure; filler metal; electron probe microanalysis (EPMA); electron backscattered diffraction (EBSD)

1 Introduction

The nickel-based Hastelloy-X superalloy with excellent high-temperature stability and extremely high corrosion and oxidation resistance is most commonly used in gas turbine engines. Additionally, MONTERO-SISTIAGA et al [1], KIM et al [2], and EKAMBARAM [3] reported that Hastelloy-X has outstanding resistance to stress corrosion cracking in an oxidizing atmosphere and would be perfect for combustion zone components. In addition, MARCHESE et al [4] expressed that it is perfectly suited for bonding methods such as welding and brazing.

JALILVAND et al [5] and EGBEWANDE et al [6] reported that transient liquid phase (TLP) bonding or diffusion bonding is a significant technique that is capable of producing almost invisible joints with similar mechanical properties and microstructure as those of the base metal. SADEGHIAN et al [7] expressed that TLP is often used where other bonding methods such as welding and brazing cannot be used for multiple reasons,

Corresponding author: A. MALEKAN, Tel: +98-9127066290, Fax: +98-21-88773352, E-mail: ahmadmalekan@gmail.com, a.malekan@merc.ac.ir
DOI: 10.1016/S1003-6326(22)65892-8

including low bonding temperature and inadequate mechanical properties, leading to the formation of brittle phases and hot cracking. GHASEMI and POURANVARI [8] and MALEKAN et al [9] expressed that TLP bonding is widely applicable to high-temperature materials such as Hastelloy-X that can be affected by incoming extreme thermal energy, and therefore, need to be bonded at low temperatures.

FARZADI et al [10] and YUAN et al [11] believe that separate steps of TLP bonding are as follows: (1) liquefying the interlayer, (2) dissolving the substrate material, (3) diffusing interlayer into the substrate and solidifying isothermally, and (4) homogenizing the bond. For producing an efficient joint, a suitable filler metal that contains melting point depressant (MPD) elements is needed. BAKHTIARI and EKRAMI [12] reported that MPD elements such as B, Si, and P reduce the melting point and diffuse rapidly into the base metal by heating up to the specific bonding temperature (T_b). ARHAMI et al [13] and DOROUDI et al [14] expressed that relative to MPD elements and the other elements in the filler metal, T_b is somehow between the solidus and liquidus lines of the base metal and filler metal phase diagram.

ARHAMI and MIRSALEHI [15] reported that to achieve the best TLP bonding joint, it is important to optimize the bonding conditions, particularly for the isothermal solidification stage, due to the mechanical and microstructural impact. ARHAMI et al [16] and MALEKI et al [17] studied the optimization of the bonding parameters. They reported that the formation of eutectic phases along the joint is inevitable if the bonding parameters are not selected appropriately to complete the isothermal solidification. Improper selection of bonding parameters could also lead to high density of precipitates in diffusion-affected zone (DAZ). These constituents are detrimental to the mechanical and corrosion-resistance properties of the joints. Moreover, GHASEMI and POURANVARI [18] examined the formation of intermetallic phases during the TLP bonding of Hastelloy-X. The effect of process temperature and duration on the mechanical properties of the bonded alloy was investigated in our previous works [9,19,20]. The effect of process parameters on the microstructure of DAZ in nickel-based superalloys has rarely been studied; further, for Hastelloy-X, this effect has not been studied in detail thus far. In the present work, the influences of holding time and filler metal thickness (joint gap) on the microstructure and microhardness of TLP-bonded Hastelloy-X, using AMS 4777 as the filler metal, have been studied. The focus of this study is on the effect of these parameters on the microstructure of the DAZ and the precipitates formed in this area.

2 Experimental

Hastelloy-X sheets with a thickness of 5 mm and AMS 4777 amorphous foils with thicknesses of 20, 35, 50, 65, and 100 μm were used as the base metal and filler metal, respectively. Table 1 lists the chemical composition of the base metal and filler metal. The filler and base metal were cut to the same dimensions of 10 mm × 10 mm using an electro discharge machine (EDM) for TLP tests. The surfaces of the base metal pieces were polished using an 800-grade SiC paper and thereafter cleaned by ultrasonic vibration in acetone solution for approximately 15 min to remove the contamination layer produced during the EDM process. Finally, each piece of the filler metal was inserted between two pieces of the base metal for the TLP tests. The joint gap was kept fixed by a stainless-steel fixture during the process. The implied pressure of 0.4 MPa was similar for all specimens.

The TLP process was performed in a vacuum furnace with the parameters listed in Table 2. Cooling of the TLP samples to room temperature was also conducted in a vacuum furnace.

Microstructural investigations were conducted via scanning electron microscopy (SEM, KEYENCE VE−8800) and electron probe microanalysis (EPMA, Shimadzu EPMA−1720) with an equipped

Table 1 Chemical composition of Hastelloy-X and AMS 4777 filler metal (wt.%)

Material	Ni	C	S	Cu	Cr	Co	Mo	Al	Ti	Si	Fe	P	Mn	B	W
Hastelloy-X	Bal.	0.08	0.001	0.02	21.21	1.13	8.84	0.16	0.02	0.36	18.16	0.007	0.46	0.003	0.54
Filler metal (AMS 4777)	Bal.	–	–	–	–	–	–	–	–	4.5	3.1	–	–	3.1	–

Table 2 TLP process parameters used in this study

Vacuum pressure/Pa	Holding temperature/°C	Holding time/min
$1.33\times(10^{-2}-10^{-3})$	1070	5−640
Filler metal thickness/μm	Heating rate/(°C·min^{-1})	
35−100	15	

ultra-thin window wavelength dispersive X-ray spectrometer (WDX) to accurately measure light elements such as boron and carbon as was suggested by RUIZ−VARGAS et al [21]. SEM (Hitachi SU8230) was also conducted along with electron backscattered diffraction (EBSD) (2 μm or 0.1 μm step size) for investigating the prepared samples. The OIM 7 software was used to perform EBSD data visualization and post processing. The prepared samples were cut from the TLP samples perpendicularly. They were then polished by SiC papers initially, thereafter by diamond abrasive (9, 6, and 1 μm), and finally, using basic colloidal silica slurries, followed by a brief vibratory polish. The etching process was performed using a solution consisting of 10 mL HNO_3, 10 mL $C_2H_4O_2$, and 15 mL HCl. Quantitative parameters like DAZ density were measured using an image analysis system (Clemex, Vision Pro. Ver. 3.5.025).

A Vickers microhardness tester was used to determine the microhardness profiles across the bonding region using a 50 g load in accordance with the ASTM standard E384 [22]. The hardness value at each point was recorded as an average of at least five measurements.

3 Results and discussion

3.1 Overall microstructure of joint and phases formed

Figure 1(a) shows the SEM micrograph of the athermally solidified zone (ASZ), isothermally solidified zone (ISZ), and DAZ after the TLP process at 1070 °C for 20 min. A high-magnification image of the ASZ area is shown in Fig. 1(b). Table 3 lists the chemical composition of the specified phases in the ASZ obtained by EPMA. The results show that the phases marked as A, B, and C are rich in nickel and boron, nickel and silicon, and chromium and boron, respectively. Based on the results of Table 3, the phases marked as D and E are Ni−Si phase (nickel silicate) and primary γ. Figure 2 shows the EBSD-SEM images of the joint area, including image quality (IQ), phase, and IPF maps.

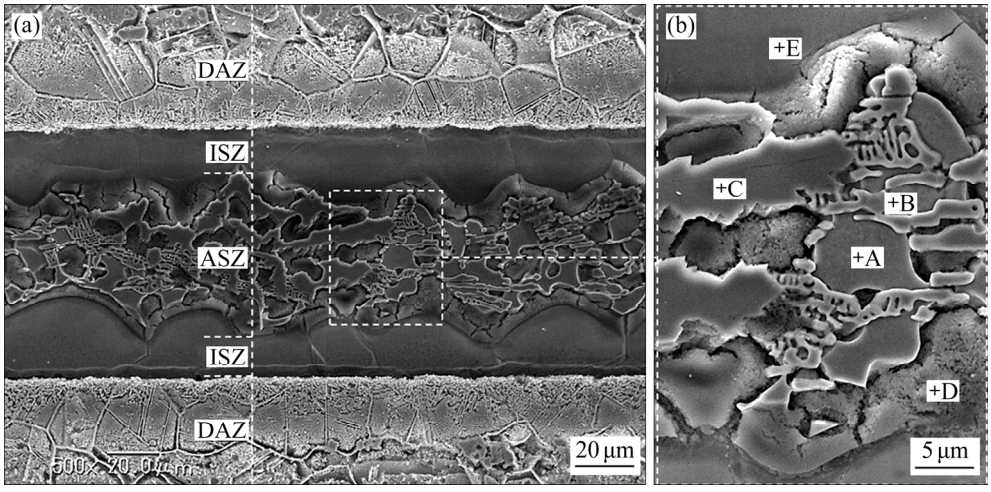

Fig. 1 SEM micrograph showing different zones of TLP joint processed at 1070 °C for 20 min with 100 μm filler metal thickness

Table 3 Chemical compositions of phases present in ASZ (Fig. 1) (at.%)

Point	Ni	Cr	Mo	Fe	Co	Si	B	C	Possible phase
A	69.74	3.62	0.01	1.98	0.00	0.19	23.85	0.61	Ni_3B
B	66.57	0.75	0.01	0.72	0.00	31.30	0.00	0.65	Ni_2Si
C	1.29	48.63	0.50	0.68	0.00	0.01	48.31	0.58	CrB
D	58.94	2.68	0.00	2.86	0.02	25.89	8.63	0.98	Nickel silicate
E	73.92	8.53	0.02	5.27	0.03	8.14	3.22	0.87	Primary γ

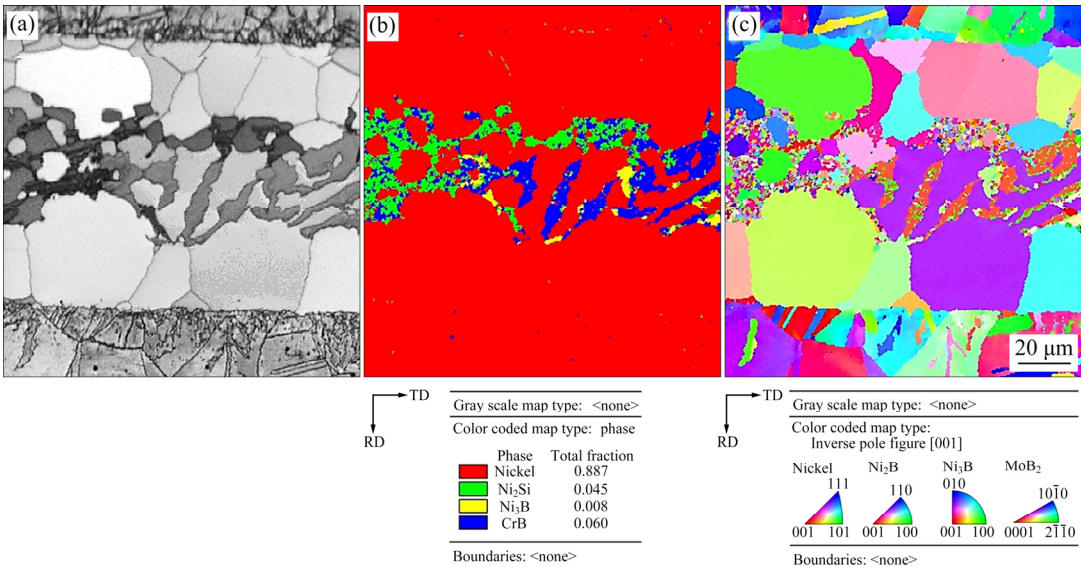

Fig. 2 EBSD-SEM images of sample with 100 μm filler metal thickness, bonded at 1070 °C for 20 min: (a) Image quality (IQ) map; (b) Phase map; (c) Inverse pole figure (IPF) map

Different areas of the ASZ, ISZ, DAZ, and base metal can be observed in Fig. 2(a). According to Fig. 2(b), the primary eutectic phases present in ASZ are Ni_3B, Ni_2Si, and CrB. The EBSD phase map (Fig. 2(b)) confirms the results of the EPMA point analysis (Table 3) and the findings of DASTGHEIB et al [23], AMIRKHANI et al [24], and LIU et al [25].

Figure 2(c) shows the EBSD orientation map of the TLP joint bonded at 1070 °C for 20 min including the inverse pole figure (IPF). Different orientations of the grains can be distinguished by dissimilar colors. The grain orientations of BM, ISZ, and ASZ are completely different due to isothermal and athermal solidification occurring in the joint area. Figure 2(a) also reveals that the grain size at the joint interface is much smaller than that in other areas. This implies that there are more grain boundaries in this area. Because the grain boundary is known to be the most preferred path for boron diffusion as was concluded by KIM et al [26], a high density of boride particles with different morphologies is observed in the DAZ (Fig. 3). The EBSD phase map results of our previous work [20] have revealed that these phases are MoB, CrB_2, and Mo_2B_5.

3.2 Effect of holding time and filler metal thickness

Figure 4 shows the TLP bonding with different filler metal thicknesses and holding time. The width of the ASZ decreases with increasing process time

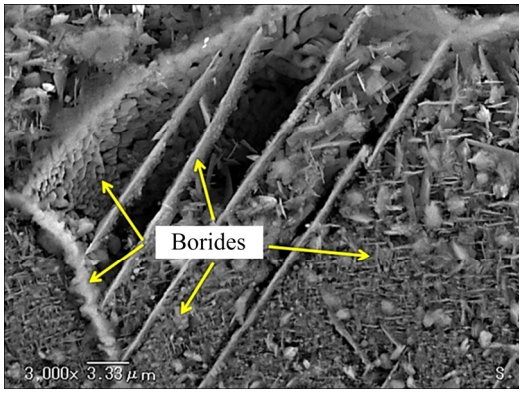

Fig. 3 SEM secondary image showing different types of borides present in DAZ

until this area is completely eliminated with the completion of the isothermal solidification process. In the 35, 50, and 65 μm-thick interlayer samples, isothermal solidification is completed in 80 min, while in the 100 μm-thick sample, more time is required. Increasing the process time also increases the DAZ width and reduces the density of borides in this area. In fact, with increasing time, boron, with its higher diffusion power, can diffuse to greater distances inside the base metal, increasing the diffusion range and reducing the density of borides in DAZ. According to Fig. 4, increasing the process time and decreasing the thickness of the interface layer can help complete the process of isothermal solidification and remove the ASZ, leading to a joint more similar to the base metal.

Figure 5 shows the density of precipitates in the DAZ with different holding time and filler metal

thicknesses. Although the density of DAZ is not changed significantly with increasing holding time up to 80 min, considerable decreases are observed for holding time of 320 and 640 min. The reduction in the density of precipitates in the 100 μm-thick sample is not high, even for holding time of 640 min. In fact, the number of borides in DAZ is large in higher thicknesses (100 μm), in which the

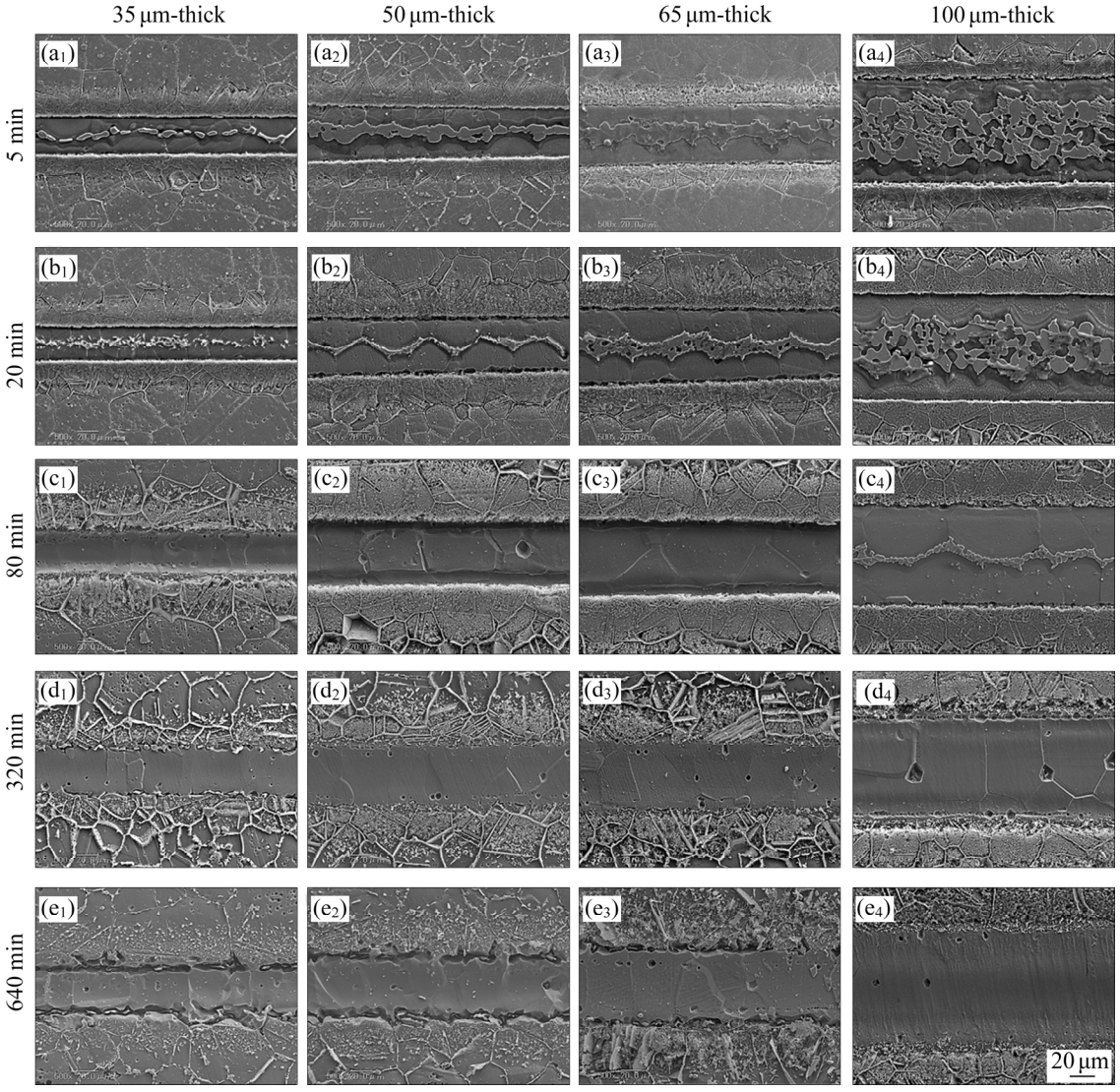

Fig. 4 TLP joints bonded with different filler metal thicknesses for different time durations

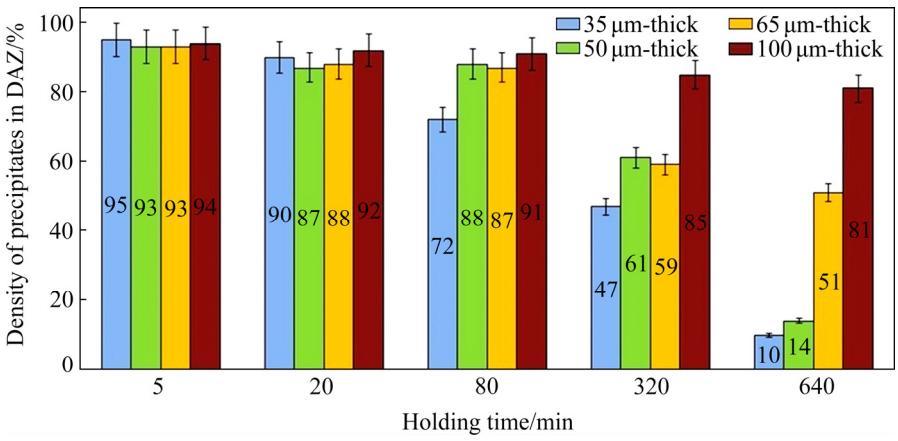

Fig. 5 Effect of holding time and filler metal thicknesses on density of precipitates in DAZ

640 min holding time is not sufficient to lead to a considerable amount of boron diffusion in order to reduce the density of precipitates in the DAZ. However, for the 35 and 50 μm-thick samples, the density is decreased to below 15% for holding time of 640 min. Therefore, increasing the holding time can help to reduce the density of precipitates in the DAZ, particularly in samples with lower filler metal thicknesses, and results in a uniform TLP joint.

Figure 6 shows the Vickers microhardness across the joint area and from the mid-line of the joints in the TLP samples with three different

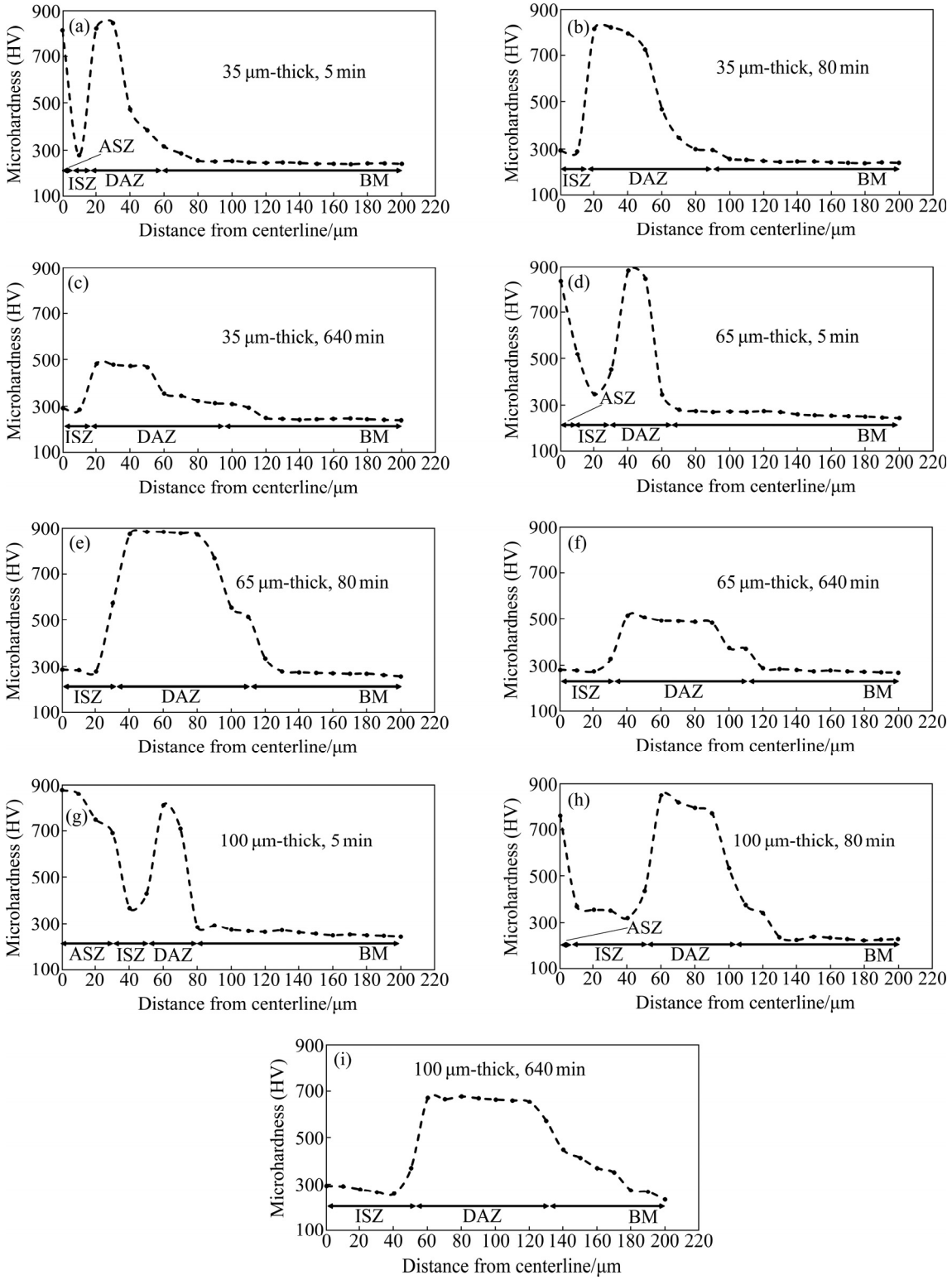

Fig. 6 Results of Vickers microhardness across joint area in samples bonded for different holding time and filler metal thicknesses

holding time and filler thicknesses. ASZ is removed by increasing the holding time from 5 to 80 min for the filler metal thickness of 35 and 65 μm. This is observed in a sample with a thickness of 100 μm, when the holding time is increased to 640 min. In general, changes in hardness during the holding time of 640 min are much less than those in the shorter holding time of 5 and 80 min, and the hardness is more uniform. It can also be seen that at a constant holding time, the degree of hardness change in the joint decreases as the thickness of the filler layer decreases. Moreover, as the phases available in the ASZ and DAZ are very hard, by reducing these zones and removing as many of these phases as possible, the hardness along the joint area is close to the base metal hardness. As shown in Fig. 4, in the given specimens with different holding time, the size of ASZ and DAZ decreases as the thickness of the interface layer decreases. Therefore, the hardness changes along the joint area are reduced with increasing holding time, and decreasing thickness of the filler layer, leading to a joint with more uniform properties.

ARAFIN et al [27] stated that the time required to complete isothermal solidification (t_f) can be calculated using the following relationship:

$$t_f = (2h)^2/(16\gamma^2 D) \quad (1)$$

where γ is a constant that accounts for the moving boundary, $2h$ is the final maximum width of the molten zone, and D is the diffusion coefficient of solute atoms into the base alloys. This relationship shows that by reducing the thickness of the interlayer and increasing the diffusion coefficients of solute atoms, the time required for isothermal solidification can be reduced. Figure 7 shows a sample jointed with a 20 μm-thick interlayer for a holding time of 5 min. In this sample, owing to the small thickness of the interlayer, even with a very short process time, the isothermal solidification process is completed. Therefore, by choosing a joint gap enough small, ASZ cannot be formed, and thus a more uniform joint can be obtained. With another model described in our previous work [19], the t_f for the sample in Fig. 7 is estimated to be 196 s, which is consistent with the experimental results explained above.

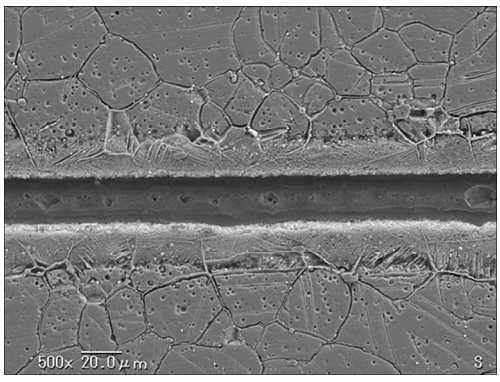

Fig. 7 SEM micrograph of TLP sample joined for 5 min with filler metal thickness of 20 μm

3.3 Detail investigation of DAZ

Figure 8 shows the SEM backscattered images and boron maps of DAZ in the Hastelloy-X/AMS 4777 TLP joints bonded at 1070 °C with a 35 μm-thick interlayer at holding time of 5 and 80 min. As shown in Fig. 8, the density of the borides in the DAZ decreases with increasing holding time. The image analysis reveals that the density of borides decreases from 22% in the sample with a holding time of 5 min to 8% in the sample with a holding time of 640 min. First, the increase in the boron diffusion distance causes the borides to accumulate over a wider range (Fig. 8(b)). The maximum diffusion range of boron into the base metal from the joint interface increases from 50 μm for the sample with holding time of 5 min to about 110 μm for the sample with holding time of 80 min. Figure 9 shows the SEM backscattered image and map analysis of DAZ for the sample with holding time of 640 min. Figure 9(b) shows that the dissolution of borides inside the base metal occurs with a large increase in the process time. JALILIAN et al [28] reported the presence of Mo_2B and MoB and that of only Mo_2B for longer holding times during transient liquid phase bonding of Inconel 617 using Ni−Si−B filler metal. However, EBSD phase map results published in our previous work [20] revealed that MoB, CrB_2, and Mo_2B_5 are the available DAZ phases of the Hastelloy-X sample bonded for 320 min. According to the B, Cr, and Mo map analysis of the sample (Figs. 9(b, c, d)), Cr-rich borides are removed at the holding time of 640 min and only the Mo-rich borides remain in the DAZ, in agreement with the results reported by JALILIAN et al [28]. The remaining borides can be classified into two types of grain boundaries and intergranular borides based on their location in the microstructure (Fig. 9(a)). Figure 10 shows the SEM micrograph and elemental map analysis of

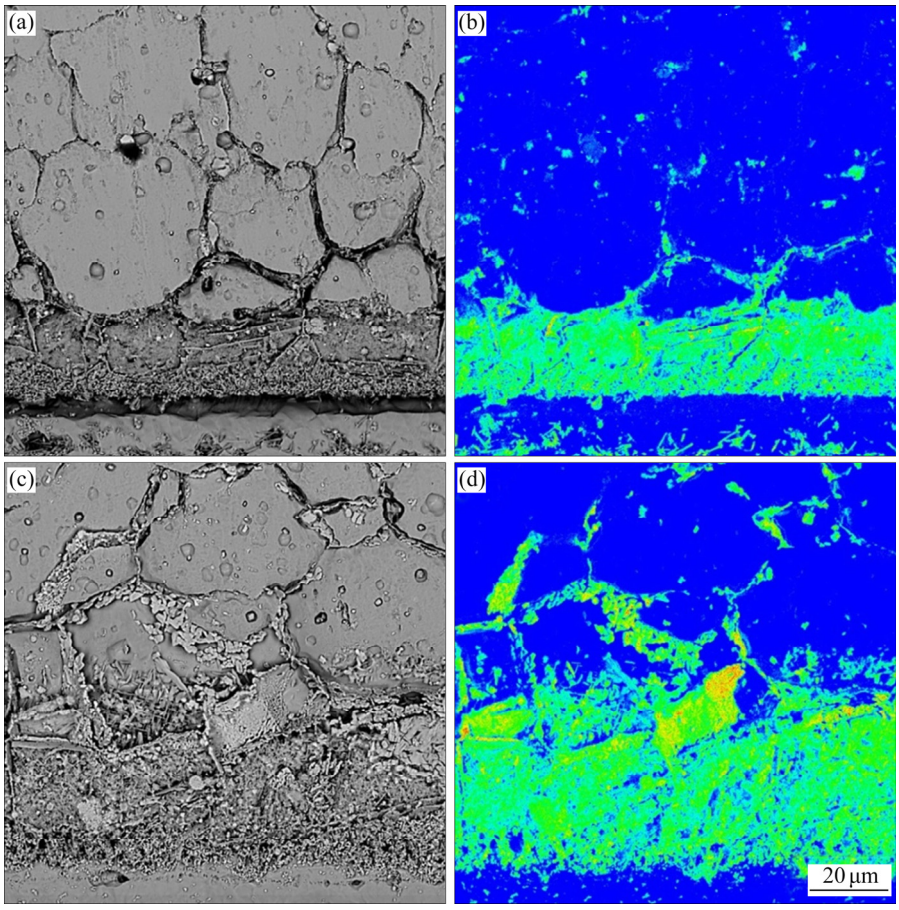

Fig. 8 SEM backscattered images (a, c) and boron maps (b, d) of DAZ in joints bonded at 1070 °C with 35 μm-thick interlayer for different holding time: (a, b) 5 min; (c, d) 80 min

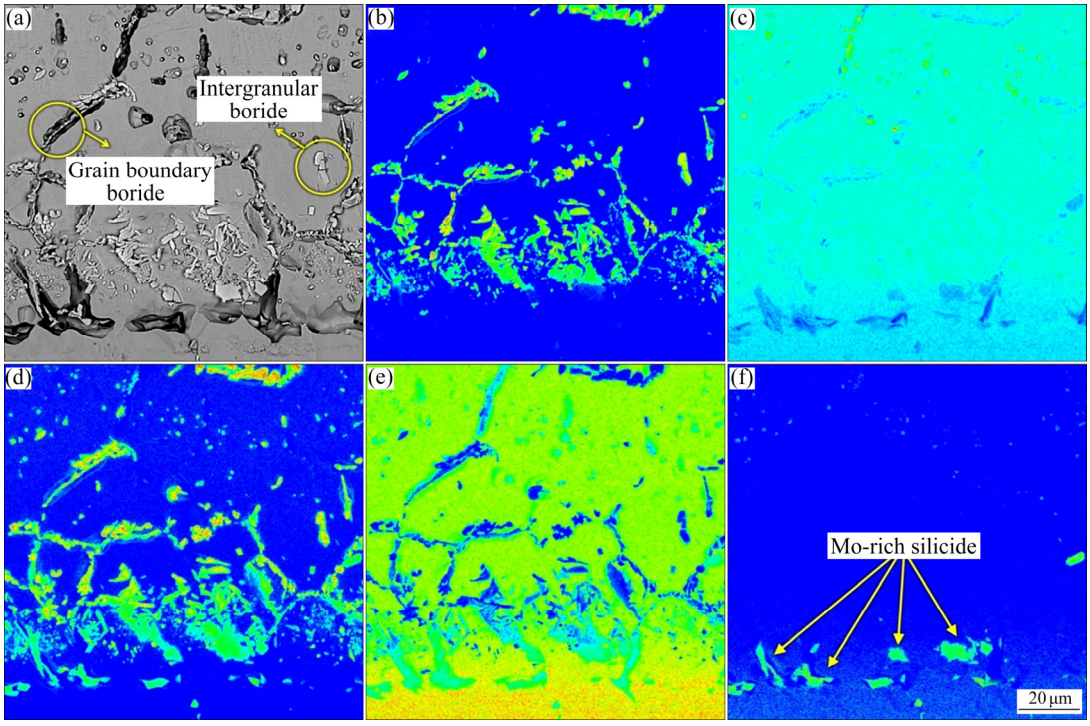

Fig. 9 SEM backscattered image (a), and map analysis of B (b), Cr (c), Mo (d), Ni (e) and Si (f) elements in DAZ of sample with holding time of 640 min

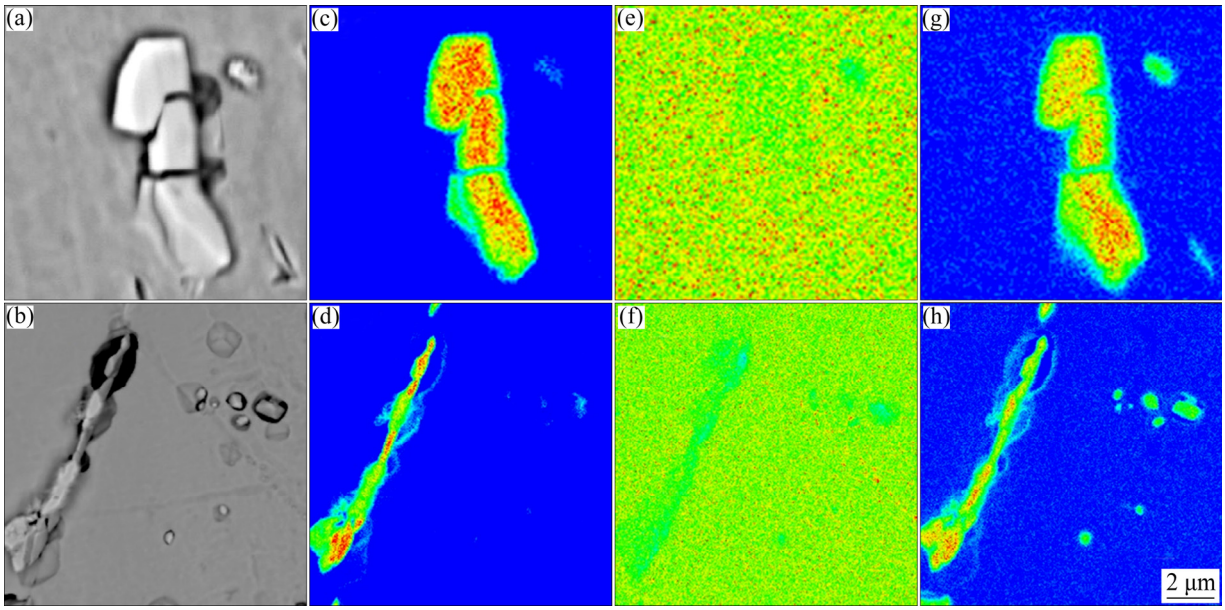

Fig. 10 SEM backscattered images of grain boundary (a) and intergranular type (b) of remnant borides, and corresponding maps of elements B (c, d), Cr (e, f) and Mo (g, h)

each of these two types. According to Fig. 10, these precipitates are rich in boron and molybdenum and have very low chromium content. GHONEIM and OJO [29] reported the high affinity of molybdenum for boron. This makes some Mo-rich borides stable even with long process time. Figure 9(f) reveals some Mo-rich silicide at the joint interface. In fact, as the process time increases, silicon is able to diffuse to long distances, and simultaneously, the amount of soluble molybdenum in the base metal increases owing to the dissolution of some Mo borides. Therefore, molybdenum and silicon interact at the joint interface and Mo-rich silicide is formed.

4 Conclusions

(1) Small filler metal thickness and long holding time encourage the isothermal solidification process and eliminate the ASZ central eutectic phases.

(2) The density of precipitates in the DAZ decreases with decreasing filler metal thickness and increasing holding time.

(3) Decrease in hardness in ASZ and DAZ due to the elimination of brittle phases in these zones during long holding time causes more uniform hardness distribution in the joint area. The best results are obtained for the sample joined with the 35 μm-thick filler metal for 640 min holding time.

(4) Isothermal solidification is completed by decreasing the filler metal thickness to 20 μm, even for the short holding time of 5 min.

(5) Studies on the DAZ precipitates reveal that Cr-rich borides are removed from DAZ with increasing holding time, and Mo-rich silicide is formed at the joint interface.

Acknowledgements

We are grateful to Associate Professor Shinji MUNETOH and Mrs. Yukiyo TAKASAKI for their assistance with EPMA analysis.

References

[1] MONTERO-SISTIAGA M L, POURBABAK S, van HUMBEECK J, SCHRYVERS D, VANMEENSEL K. Microstructure and mechanical properties of Hastelloy X produced by HP-SLM (high power selective laser melting) [J]. Material and Design, 2019, 165: 107598.

[2] KIM W G, YIN S N, RYN W S, CHANG J H, KIM S J. Tension and creep design stresses of the “Hastelloy-X” alloy for high-temperature gas cooled reactors [J]. Materials Science and Engineering A, 2008, 483/484: 495−497.

[3] EKAMBARAM P. Study of mechanical and metallurgical properties of Hastelloy X at cryogenic condition [J]. Materials Research and Technology, 2019, 8: 6413−6419.

[4] MARCHESE G, BASILE G, BASSINI E, AVERSA A, LOMBARDI M, UGUES D, FINO P, BIAMINO S. Study of the microstructure and cracking mechanisms of Hastelloy X produced by laser powder bed fusion [J]. Materials (Basel), 2018, 11: 106.

[5] JALILVAND V, OMIDVAR H, SHAKERI H R, RAHIMIPOUR M R. Microstructural evolution during transient liquid phase bonding of Inconel 738LC using AMS 4777 filler alloy [J]. Materials Characterization, 1970, 75: 20−28.

[6] EGBEWANDE A T, CHUKWUKAEME C, OJO O A. Joining of superalloy Inconel 600 by diffusion induced isothermal solidification of a liquated insert metal [J]. Materials Characterization, 2008, 59: 1051−1058.

[7] SADEGHIAN A, ARHAMI F, MIRSALEHI S E. Phase formation during dissimilar transient liquid phase (TLP) bonding of IN939 to IN625 using a Ni−Cr−Fe−Si−B interlayer [J]. Manufacturing Processes, 2019, 44: 72−80.

[8] GHASEMI A, POURANVARI M. Microstructural evolution mechanism during brazing of Hastelloy X superalloy using Ni−Si−B filler metal [J]. Science and Technology of Welding and Joining, 2018, 23: 441−448.

[9] MALEKAN A, FARVIZI M, MIRSALEHI S E, SAITO N, NAKASHIMA K. Influence of bonding time on the transient liquid phase bonding behavior of Hastelloy X using Ni−Cr−B−Si−Fe filler alloy [J]. Materials Science Engineering A, 2019, 755: 37−49.

[10] FARZADI A, ESMAIELI H, MIRSALEHI S E. Transient liquid phase bonding of Inconel 617 superalloy: Effect of filler metal type and bonding time [J]. Welding in the World, 2019, 63: 191−200.

[11] YUAN Lin, XIONG Jiang-tao, DU Ya-jie, REN Jin, SHI Jun-miao, LI Jing-long. Microstructure and mechanical properties in the TLP joint of FeCoNiTiAl and Inconel 718 alloys using BNi2 filler [J]. Materials Science and Technology, 2021, 61: 176−185.

[12] BAKHTIARI R, EKRAMI A. Transient liquid phase bonding of FSX-414 superalloy at the standard heat treatment condition [J]. Materials Characterization, 2012, 66: 38−45.

[13] ARHAMI F, MIRSALEHI S E, SADEGHIAN A, JOHAR M H. The joint properties of a high-chromium Ni-based superalloy made by diffusion brazing: Microstructural evolution, corrosion resistance and mechanical behavior [J]. Manufacturing Processes, 2019, 37: 203−211.

[14] DOROUDI A, SHAMSIPOUR A, OMIDVAR H, VATANARA M. Effect of transient liquid phase bonding time on the microstructure, isothermal solidification completion and the mechanical properties during bonding of Inconel 625 superalloy using Cr−Si−B−Ni filler metal [J]. Manufacturing Processes, 2019, 38: 235−243.

[15] ARHAMI F, MIRSALEHI S E. Microstructural evolution and mechanical properties evaluation of IN-939 bonds made by isothermal solidification of a liquated Ni−Cr−B interlayer [J]. Metallurgical and Materials Transactions A: Physical Metallurgy and Materials Science, 2018, 49: 6197−6214.

[16] ARHAMI F, MIRSALEHI S E, SADEGHIAN A. Effect of bonding time on microstructure and mechanical properties of diffusion brazed IN-939 [J]. Materials Processing Technology, 2019, 265: 219−229.

[17] MALEKI V, OMIDVAR H, RAHIMIPOUR M R. Effect of gap size on microstructure of transient liquid phase bonded IN-738LC superalloy [J]. Transactions of Nonferrous Metals Society of China, 2016, 26: 437−447.

[18] GHASEMI A, PORANVARI M. Intermetallic phase formation during brazing of a nickel alloy using a Ni−Cr−Si−Fe−B quinary filler alloy [J]. Science and Technology of Welding and Joining, 2019, 24: 342−351.

[19] MALEKAN A, FARVIZI M, MIRSALEHI S E, SAITO N, NAKASHIMA K. Effect of bonding temperature on the microstructure and mechanical properties of Hastelloy X superalloy joints bonded with a Ni−Cr−B−Si−Fe interlayer [J]. Manufacturing Processes, 2019, 47: 129−140.

[20] MALEKAN A, FARVIZI M, MIRSALEHI S E, SAITO N, NAKASHIMA K. Holding time influence on creep behavior of transient liquid phase bonded joints of Hastelloy X [J]. Materials Science Engineering A, 2020, 772: 138694.

[21] RUIZ-VARGAS J, SIREDEY N, NOYREZ P, MATHIEU S, BOCHER P, GEY N. Potential and limitations of microanalysis SEM techniques to characterize borides in brazed Ni-based superalloys [J]. Materials Characterization, 2014, 94: 46−57.

[22] ASTM Standard E384-17. Standard test method for microindentation hardness of materials [S]. ASTM International, 2017.

[23] DASTGHEIB A, RAJABI A, OMIDVAR H. Effect of the isothermal solidification completion on the mechanical properties of Inconel 625 transient liquid phase bond by changing bonding temperature [J]. Integrative Medicine Research, 2020, 9: 10355−10365.

[24] AMIRKHANI A, BEIDOKHTI B, SHIRVANI K, RAHIMIPOUR M R. Two-step heating transient liquid phase bonding of Inconel 738LC [J]. Materials Processing Technology, 2019, 266: 1−9.

[25] LIU Ji-de, TAO Jin, ZHAO Nai-ren, WANG Zhi-hui, SUN Xiao-feng, GUAN Heng-rong, HU Zhuang-qi. Microstructural study of transient liquid phase bonded DD98 and K465 superalloys at high temperature [J]. Materials Characterization, 2011, 62: 545−553.

[26] KIM J K, PARK H J, SHIM D N, KIM D J. Transient liquid phase bonding of γ'-precipitation strengthened Ni based superalloys for repairing gas turbine components [J]. J Manufacturing Processes, 2017, 25: 60−69.

[27] ARAFIN M A, MEDRAJ M, TURNER D P, BOCHER P. Transient liquid phase bonding of Inconel 718 and Inconel 625 with BNi-2: Modeling and experimental investigations [J]. Materials Science and Engineering A, 2007, 447: 125−133.

[28] JALILIAN F, JAHAZI M, DREW R A L. Microstructural evolution during transient liquid phase bonding of Inconel 617 using Ni−Si−B filler metal [J]. Materials Science and Engineering A, 2006, 423: 269−281.

[29] GHONEIM A, OJO O A. Microstructure and mechanical response of transient liquid phase joint in Haynes 282 superalloy [J]. Materials Characterization, 2011, 62: 1−7.

焊料厚度和保温时间对瞬间液相连接 Hastelloy-X 合金接头显微组织演化的影响

A. MALEKAN[1], S. E. MIRSALEHI[2], M. FARVIZI[1], N. SAITO[3], K. NAKASHIMA[3]

1. Ceramic Division, Materials and Energy Research Center, P.O. Box 14155-4777, Tehran, Iran;
2. Department of Materials and Metallurgical Engineering,
Amirkabir University of Technology (Tehran Polytechnic), Tehran 15875-4413, Iran;
3. Department of Materials Science and Engineering, Kyushu University, 744, Motooka, Nishi-ku,
Fukuoka 819-0395, Japan

摘　要：研究不同焊料厚度(20, 35, 50, 65, 100 μm) 和保温时间(5, 20, 80, 320, 640 min)下 Hastelloy-X 样品的瞬间液相(Transient liquid phase, TLP)连接，以获得最优连接参数。电子探针显微分析(EPMA)和电子背散射衍射(EBSD)显微组织分析表明，非热凝固区(ASZ)中心的共晶相为 Ni_3B、Ni_2Si 和 CrB，扩散影响区(DAZ)形成 MoB、CrB_2 和 Mo_2B_5 析出相。结果表明，减小焊料厚度、增加保温时间有助于完成等温凝固、降低 DAZ 中析出相的密度，这使接头性能更加均匀。随着保温时间的增加，硼和硅的扩散距离变长，导致 DAZ 中富 Cr 硼化物消除，并在接头界面形成富 Mo 硅化物。随着保温时间的延长，ASZ 和 DAZ 中脆性相的消除导致其硬度降低，使得接头区域的硬度分布更加均匀。最优连接参数为：金属焊料厚 35 μm，保温时间 640 min。

关键词：Hastelloy-X；瞬间液相(TLP)连接；显微组织；焊料；电子探针显微分析(EPMA)；电子背散射衍射(EBSD)

(Edited by Bing YANG)